Journal of Robotics and Control (JRC)
Volume 5, Issue 1, 2024
ISSN: 2715-5072, DOI: 10.18196/jrc.v5i1.20705

A Performance Evaluation of Repetitive and Iterative Learning Algorithms for Periodic Tracking Control of Functional Electrical Stimulation System

Edi Kurniawan [1*], Enggar B. Pratiwi [2], Hendra Adinanta [3], Suryadi [4], Jalu A. Prakosa [5], Purwowibowo [6], Sensus Wijonarko [7], Tatik Maftukhah [8], Dadang Rustandi [9], Mahmudi [10]
[1, 2, 4, 5, 6, 7, 8, 9] Research Center for Photonics, National Research and Innovation Agency, South Tangerang 15314, Indonesia
[3] Research Center for Hydrodynamics Technology, National Research and Innovation Agency, Surabaya 60112, Indonesia
[10] Research Center for Testing Technology and Standard, National Research and Innovation Agency, South Tangerang 15314, Indonesia
Email: [1] edik004@brin.go.id, [2] enggarbpratiwi@gmail.com, [3] hendra.adinanta@brin.go.id, [4] sury023@brin.go.id, [5] jalu.ahmad.prakosa@brin.go.id, [6] purw001@brin.go.id, [7] sens001@brin.go.id, [8] tati006@brin.go.id, [9] dad003@brin.go.id, [10] mahm004@brin.go.id
*Corresponding Author

***Abstract*—Functional electrical stimulation (FES) is a medical device that delivers electrical pulses to the muscle, allowing patients with spinal cord injuries to perform activities such as walking, cycling, and grasping. It is critical for the FES to generate stimuli with the appropriate controller so that the desired movements can be precisely tracked. By considering the repetitive nature of the movements, the learning-based control algorithms are utilized for regulating the FES. Iterative learning control (ILC) and repetitive control (RC) are two learning algorithms that can be used to accomplish accurate repetitive motions. This study investigates a variety of ILC and RC designs with distinct learning functions; this constitutes our contribution to the field. The FES model of ankle angle, which is in a class of discrete-time linear systems is considered in this study. Two learning functions, i.e., proportional, and zero-phase learning functions, are simulated for the second-order FES model running at a sampling time of 0.1 s. The results indicate the superior performance of the ILC and RC in terms of convergence rate using the zero-phase learning function. ILC and RC with a zero-phase learning function can reach a zero root-mean-square error in two iterations if the model of the plant is correct. This is faster than proportional-based ILC and RC, which takes about 40 iterations. This indicates that the zero-phase learning function requires two iterations to ensure that the patient's ankle angle precisely tracks the intended trajectory. However, the tracking performance is degraded for both control methods, especially when the model is subject to uncertainties. This specific problem can lead to future research directions.**

Keywords—Perfect Tracking; Repetitive Control; Iterative Learning Control; Learning Function; Functional Electrical Simulation.

I. INTRODUCTION

Tracking control problems have been found in many biomedical applications such as wearable lower-limb system [1], [2], magnetoactive soft continuum robots (MSCRs) [3], pneumatic artificial muscles [4], [5], [6], [7], mimic the intact human knee profile [8], simple magnetically actuated pivot walker [9]. Similarly, tracking control problems also appeared on robotic arm [10], multi-input multi-output (MIMO) drug infusion [11], grasping ability hands robot [12], leg hydraulic drive system (LHDS) [13], pneumatic soft robotic actuator [14], and functional electrical stimulation (FES) [15], [16]. Recently, tracking control of FES has gained much attention due to its benefits and challenges for regulating the movements of people with Spinal Cord Injury (SCI). SCI commonly happens because of the neural tissue defects that make partial or complete loss of sensory functions. Here, FES was generally used for helping people with SCI in order to improve their motor functions. Therefore, FES can assist people with SCI to do daily movements such as walking, standing, grasping, and cycling, which are iterative in nature. In principle, FES sends electrical pulses to the muscles. These electrical pulses trigger muscle contractions that exert a torque about the joints. The intensity, period and frequency of stimulation provided to the muscles can be modulated to control the joint angle. In simple terms, the joint angle (i.e. plant output) can be controlled by manipulating one of the following FES variables: (a) pulse width, (b) pulse amplitude, or (c) stimulation frequency to achieve accurate iterative motions. FES can be controlled using one of two general control structures: open-loop or closed-loop. Open-loop FES becomes a common system that uses a feedforward mechanism, which has a disadvantage. Continuous user input is compulsory for this open-loop FES; therefore, the user must maintain complete focus while operating the FES device [15].

In vice versa, a closed-loop FES system uses a feedback mechanism to correct the actual joint angle. Thus, a closed-loop demands less user interaction compared to the open-loop FES system. Some research works related on the design of closed-loop FES systems can be found in [17]–[23]. A distributed cooperative control utilizing an adaptive higher-order sliding mode (AHOSM) control method was developed in [17] to simultaneously control of torque and cadence during FES-cycling. A closed-loop FES controller for compensating time-varying, nonlinear, uncertain dynamics and the unknown time-varying muscle delay (electromechanical delay) was proposed [18]. The work [19]

developed a closed-loop FES-based control solution for gait rehabilitation based on a finite state machine (FSM) model. A control strategy combining robust sliding-mode and adaptive admittance control schemes was designed for controlling the rider's muscles and the cycle's motor in order to maintain comfort and safety [20]. The work [21] developed a Lyapunov-based velocity tracking control of recumbent trike with FES. A model predictive control for tracking human limb angle with FES and an electric motor assist was investigated in [22]. To reduce the amount of required control signal, the authors [23] employed an integral concurrent learning (ICL) controller during motorized and FES-induced biceps curls. The work [24] designed a bilateral control technique of shoulder and elbow joints using FES between human and 3 DoF robot.

The above closed-loop FES systems can be classified as non-predictive control systems. The above-mentioned non-predictive control systems such as sliding mode control (SMC) and adaptive control can be classified as robust control approaches aiming to handle model uncertainties and to compensate for some disturbances. Based on the studies in [25]–[29], the performances of such as SMC and adaptive control-based schemes are inferior for tracking/rejection periodic signal compared to predictive-based control methods. This is due to the above controlled systems do not have capability to learn from the previous error and use it to refine the current control signal. Another possible control approach that can be used for the above purpose (e.g., swinging the ankle repeatedly) is learning control algorithms. Learning control is a control strategy capable of learning from the previous error to refine the current control signal to improve the controlled system's performance. In this case, learning control is relevant and advantageous for achieving high accuracy tracking for the systems doing repetitive motions. The learning algorithm here refers to two control schemes: Iterative Learning Control (ILC) and Repetitive Control (RC). Both ILC and RC have been used in many industrial applications due to their performance to achieve high accuracy tracking.

This article evaluates the tracking capabilities of ILC and RC, which are both employed to regulate FES for stimulating ankle joint to follow iterative trajectory. Multiple ILC and RC controller designs are simulated for the FES model of ankle angle, which is in the class of discrete-time linear systems. The tracking performance of the presented control techniques are analyzed and discussed. The contributions of this work are then listed as follows:

- The tracking performance of both ILC and RC is assessed for controlling FES. This is important since FES has repetitive behavior, while ILC and RC are known to work best for systems doing repetitive motions.
- Two distinct learning functions, namely, proportional, and zero-phase learning functions are examined for both ILC and RC closed-loop systems to show the convergence rate for reaching a zero-tracking error.
- Additionally, the tracking performance of ILC and RC is also assessed in the case that the FES system is subject to model inaccuracies.

The rest of this work is organized as follows: Section 2 discusses the Method covering FES model, problem formulation, ILC and RC designs. Problem formulation is necessary to emphasize the class of plant model and some assumptions used throughout this research work. Section 3 presents the simulation results and discussion, and Section 4 concludes this work.

II. METHOD

A. FES Model and Control Variables

In this study, FES is an object to be controlled. FES is a device that uses electrodes attached to the skin to transmit a series of electrical pulses to neurons. Because of receiving electrical pulses, muscle contractions are generated. The stimulation pulse is a biphasic square-wave pulse train with a frequency of $20 - 40$ Hz, an amplitude of $0 - 120$ mA, and a pulse duration of $0 - 300$ μs [15]. The use of this biphasic waveform makes the induced charge transferred into the tissue, will be immediately transferred out of the tissue. FES system can produce titanic contractions by stimulating the motor at a frequency $20 - 40$ Hz. The intensity and frequency of electrical stimulation affect the tension produced in electrically activated muscle. Thus, the joint angle or torque can be controlled by varying one of the following variables: (a) pulse amplitude, (b) pulse duration, or (c) stimulation frequency.

Let consider a discrete-time linear time invariant (LTI) system representing the FES model as follows:

$$y(k) = P(z)u(k), \tag{1}$$

where $u(k) \in \mathbb{R}$ is a control input (pulse width), $y(k) \in \mathbb{R}$ is a plant output (ankle joint angle), and $P(z)$ is a plant (FES) model.

The plant model $P(z)$ is formulated by:

$$P(z) = z^{-m}\frac{b_0 + b_1 z^{-1} + \cdots + b_{p-m} z^{-p+m}}{1 + a_0 z^{-1} + \cdots + a_p z^{-p}}, \tag{2}$$

where p and m are an order and the relative degree of the plant respectively, $b_0, b_1, \cdots, b_{p-m}$ are plant numerator's coefficients, $a_0, a_1, \cdots, a_p$ are plant denominator's coefficients.

The plant model (2) is assumed to be a stable minimum phase plant with an order p and relative degree m. The LTI system (1) has an equivalent state-space form as follows:

$$\begin{aligned} x(k+1) &= Ax(k) + Bu(k) \\ y(k) &= \mathrm{C}x(k), \end{aligned} \tag{3}$$

where $\mathrm{x}(k) \in \mathbb{R}^p$ is a discrete-time state vector, A is $p \times p$ system matrix, B is $p \times 1$ input matrix, and C is $1 \times p$ output matrix. The matrices A, B, and C are constructed based on the coefficients in (2), and given as (4).

$$\mathrm{A}=\begin{bmatrix}-a_0 & -a_1 & \cdots & -a_p\\ 1 & 0 & 0 & 0\\ 0 & 1 & 0 & 0\\ 0 & 0 & 1 & 0\end{bmatrix},\mathrm{B}=\begin{bmatrix}1\\0\\0\\0\end{bmatrix},\mathrm{C}=\begin{bmatrix}b_0\\ \vdots\\ b_{p-m}\\ 0\end{bmatrix}^T \quad (4)$$

Consider that the trajectory to be tracked or the reference $y_R(k)$, is a repetitive signal with known period T_r, and assume that the plant model (2) is accurately known, then our control objective is to generate control input $u(k)$ in (1) such that the plant output $y(k)$ perfectly follow the reference $y_R(k)$, and such that the tracking error $e(k)$, $e(k)=y_R(k)-y(k)$, asymptotically converges to zero. To achieve the above objective, we consider two control approaches, namely Iterative Learning Control (ILC) and Repetitive Control (RC) designs as detailed in next subsections.

B. ILC Design

Iterative Learning Control (ILC) is a widely recognized control approach that is commonly used for systems that perform similar tasks repeatedly. An ILC algorithm was introduced by Arimoto [30], and it was used for controlling robots doing repetitive movements. ILC has been applied in many control applications such as high-speed trains [31]–[33], hydraulic cushion [34], walking piezo actuators (WPA) [35], fault estimation (FE) [36], twin-roll strip casting [37], crane system [38], electron linear accelerator [39], tank gun control system [40], monocrystalline batch process [41], nano-positioning stage [42], fractional-order multi-agent systems (FOMASs) [43], robotic manipulator [44], [45], [46], robotic path learning [47], magnetically levitated (maglev) planar motor [48], model uncertainties [49], autonomous farming vehicle [50], unmanned vehicle [51], additive manufacturing system [52], and marine hydrokinetic energy system [53]. A general ILC system has an architecture as shown in Fig. 1. An ILC is based on the idea that by learning from past iterations, the performance of a system that performs the same task several times can be improved. Note that the previous iteration values of both the tracking error e_j and control signal u_j are stored in memory.

The ILC runs by producing and executing the control input per iteration (also known as trial/batch/repetition/period), where each iteration consists of a finite number of samples (sequences). Let assume that each iteration is uniform having fixed period of T_r. Then, the number of sequences N is also constant given by $N=T_r/T$, where T is sampling period. Consider we have $N-$ sequences per iteration, then we can write control input $u(k)$,

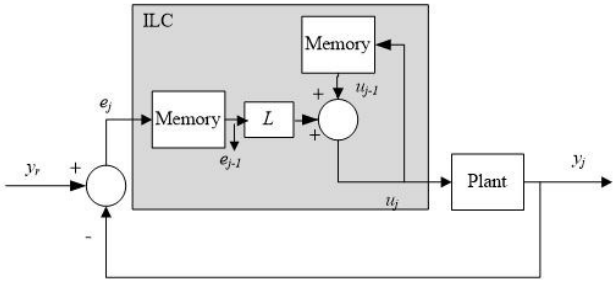

Fig. 1. A generic discrete-time ILC system architecture

plant output $y(k)$, and the reference signal $y_R(k)$ of the ILC system as follow:

$$U_j=\left[u_j(0),u_j(1),\cdots,u_j(N-1)\right]^T, U_j\in\mathbb{R}^N \quad (5)$$

$$Y_j=\left[y_j(m),y_j(1),\cdots,y_j(N-1+m)\right]^T, Y_j\in\mathbb{R}^N \quad (6)$$

$$Y_{Rj}=\left[y_{rj}(m),y_{rj}(1),\cdots,y_{rj}(N-1+m)\right]^T, Y_{Rj}\in\mathbb{R}^N \quad (7)$$

where $\{0,1,2,3,\cdots,N-1\}$ are step indices for control input, $\{m,m+1,\cdots,N+m\}$ step indices for both plant output and reference signal, and $j=1,2,3,\cdots,\infty$ is the iteration number.

A general iterative learning control law combines the previous iteration values of both U_j and E_j. The control law of ILC is shown below

$$U_j=U_{j-1}+LE_{j-1}, \quad (8)$$

where U_j is control signal sequences at current iteration j, U_{j-1} is control signal sequences at previous iteration $j-1$, L is the learning matrix, and $E_{j-1}$is tracking error sequences at previous iteration $j-1$. The tracking error E_{j-1} is formulated as follows:

$$E_{j-1}=Y_R-Y_{j-1}. \quad (9)$$

Given the control law (8), the plant output sequences at iteration j is obtained from

$$Y_j=HU_j, \quad (10)$$

where H is matrix of rank N whose elements are Markov parameters of the plant model (2).

$$H=\begin{bmatrix}h_m & 0 & 0 & 0\\ h_{m-1} & h_m & 0 & 0\\ \vdots & \cdots & h_m & 0\\ h_{m+N-1} & \cdots & h_{m+1} & h_m\end{bmatrix}. \quad (11)$$

For a given state-space (3), the Markov parameter h_m can be obtained from

$$h_m=\mathrm{CA}^{m-1}\mathrm{B}, \quad (12)$$

where matrices $\mathrm{A},\mathrm{B},\mathrm{C}$ state-space matrices given in (4) and assumed to be known. Here, a scalar m represents the relative degree of plant and is given in (2). Hence, ILC system runs by generating control signal sequences U_j (8), then feeding U_j to the plant model (2) to obtain the output sequences Y_j (10).

The variable L in (8) is learning matrix originated from learning function $L(z)$. The ILC design can be seen as the selection of the learning function $L(z)$, where $L(z)$ is given by the following impulse response (13).

$$L(z) = \cdots + l_{-1}z^1 + l_0 + l_{-1}z^{-1} + \cdots \quad (13)$$

The learning matrix L can be constructed based on (13) to form a Toeplitz matrix as follows:

$$L = \begin{bmatrix} l_0 & l_{-1} & \cdots & l_{-(N-1)} \\ l_1 & l_0 & \cdots & l_{-(N-2)} \\ \vdots & l_1 & \ddots & \vdots \\ l_{-(N-1)} & \cdots & l_1 & l_0 \end{bmatrix}. \quad (14)$$

The choice of the L matrix can be thought of as the ILC design problem. Learning matrix L in (14) can be designed in several forms e.g. [54]:

1. The matrix L forms a diagonal matrix, which is called as Type A learning function. This learning function is also referred to proportional learning function that is equated by:

$$L_p = \begin{bmatrix} \gamma & 0 & 0 & 0 \\ 0 & \gamma & 0 & 0 \\ \vdots & 0 & \ddots & 0 \\ 0 & \dots & 0 & \gamma \end{bmatrix}, L_p \in \mathbb{R}^{N\times N}, \quad (15)$$

where γ corresponds to the proportional learning gain. This learning function may be regarded as the most basic design in ILC due to the fact that it solely selects the proportional gain γ without necessitating the utilization of the plant model.

2. The matrix L forms a symmetrical band diagonal matrix, which is later named as Type B learning function. This learning function is then denoted as a zero-phase learning function, and formulated by:

$$L_{zp} = \begin{bmatrix} 1/b_m & 0 & 0 & 0 & \cdots & 0 \\ a_0/b_m & 1/b_m & 0 & 0 & \cdots & 0 \\ \vdots & a_0/b_m & 1/b_m & 0 & 0 & \vdots \\ a_p/b_m & \vdots & \ddots & \ddots & \ddots & 0 \\ 0 & \ddots & \vdots & a_0/b_m & 1/b_m & 0 \\ 0 & 0 & a_p/b_m & \cdots & a_0/b_m & 1/b_m \end{bmatrix}, \quad (16)$$

$$m < N, L_{zp} \in \mathbb{R}^{N\times N}$$

The learning matrix L must be chosen carefully when designing an ILC control system. The learning matrix L determines the boundedness of the input and output signals. It also determines the tracking error's transient response and the convergence rate. An ILC system with control law (8) is asymptotically stable if only if [55].

$$\rho(I - LH) < 1 \quad (17)$$

where I is identity matrix, and $\rho(I - LH)$ is the spectral radius of matrix $(I - LH)$, which is equivalent to

$$\rho(I - LH) = max\{|\lambda_1|, |\lambda_2|, \cdots, |\lambda_N|\}. \quad (18)$$

Note that L is equivalent to L_p and L_{zp} depend on which learning function is used. The notation λ refers to the eigenvalue of matrix $(I - LH)$. The nature of ILC design is choosing L which minimizes (19). ILC design problem is generally about the selection of learning matrix L such the condition (13) is satisfied, and such that a faster convergence rate and zero-tracking error are achievable. Here, root-mean-square error (RMSE) is utilized to assess the tracking accuracy performance. The RMSE is formulated by

$$RMSE_j = \sqrt{\frac{1}{N}\sum_{k=1}^{N}\left(y_{rj}(k) - y_j(k)\right)^2}, \quad (19)$$

where $RMSE_j$ corresponds to the root mean-squared error at iteration j. The root mean-squared error (RMSE) is used in the evaluation because it offers an error measure in the same unit as the objective variable, which facilitates easy comparisons and interpretations. Furthermore, larger errors are penalized significantly by RMSE compared to mean-squared error (MSE).

In the next subsection, we present other learning-based control algorithms regarded as RC. The command to be executed in the RC system is a periodic function of time, and the system does not return to its initial state. Changes in control actions made near the completion of one period can influence the error at the beginning of the following period, and transients on RC can spread to the next repetition. As a result, the real stability boundary of ILC and RC differs significantly.

C. RC Design

Another control method for perfect tracking of repetitive trajectory is called Repetitive Control (RC). Recently, RC has been used for leg exoskeleton control [56], 1-DOF Lagrangian system [57], industrial wide-format printing [58], contouring control of micro-stereolithography [59], magnetically suspended rotor system [60], [61], [62], control of linear actuator [63], functional electrical stimulation [64], [65], grid-connected inverters [66], [67], [68], [69], [70], nanometer-order contouring [71], dynamical galvanometer-based raster scanning [72], atomic force microscopy (AFM) scanner [73], mechanical ventilation [74], permanent magnet synchronous motor (PMSM) [75]–[77], servo motor [78], plug-in electric vehicle (PEV) charger [79], piezoelectric nano positioning stage [80], hydraulic press system [81], robotic manipulator [82], [83], and electric spring [84]. The RC is based on the idea of internal model principle by Francis and Wonham [85] stated that by incorporating model of reference/disturbance then perfect reference tracking or disturbance rejection can be achieved. The general RC system has a structure as shown in Fig. 2.

RC uses N-steps time-delay with positive feedback. Learning function $L(z)$ is also employed as part of RC system. This learning function behaves as compensator which determines the system stability, transient behavior, and convergence rate of the tracking error.

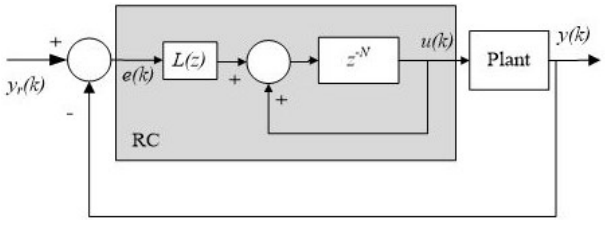

Fig. 2. A generic discrete-time RC system architecture

The general RC shown in Fig. 2 has the following transfer function:

$$\frac{\mathrm{U(z)}}{E(z)} = \frac{\mathrm{z^{-N}}}{1-\mathrm{z^{-N}}}L(z), \tag{20}$$

where $N = T_r/T \in \mathbb{N}$, N being the number of samples per iteration, T_r being the length of iteration (e.g., period of the reference signal), T being the sampling period, and N is an integer value. Note that we also assume that N is also fixed per iteration, meaning that the length of iteration T_r is also constant. This becomes a basic assumption in the design of RC.

Equation (20) can be rewritten to RC control law as follows:

$$U(k) = u(k-N) + L(z)e(k-N). \tag{21}$$

We can notice that RC control law has a similar structure to ILCs where they require past values of both control signal and tracking error. The differences are that RC is executed per sample and the system initial conditions are not reset-ed when the next iteration is started.

RC system with control law (21) and plant model (2) is asymptotically stable, if the following conditions are fulfilled [86],[87]:

1. The plant model (2) is stable.
2. The learning function $L(z)$ satisfies

$$\|1 - L(z)P(z)\|_\infty < 1, \tag{22}$$

where notation $\|.\|_\infty$ refers to the infinity norm.

Note that in the presence of model uncertainties $\Delta(z)$, which is bounded by $\|\Delta(z)\|_\infty < \delta$, then $L(z)$ is required to meet:

$$\|1 - L(z)P(z)[1+\Delta(z)]\|_\infty < 1, \tag{23}$$

which is also equivalent to

$$|1 - L(z)P(z)[1+\Delta(z)]| < 1, \forall\, \mathrm{z} = e^{j\omega}. \tag{24}$$

Here, the notation $|X(z)|$ denotes the magnitude of the transfer function $X(z)$ at $0 < \omega < {}^{\pi}/_{T}$. The model uncertainties $\Delta(z)$ makes the left-hand side of (23) and (24) becoming larger implying that the asymptotic convergence can be slower but remains stable and bounded as long as the value is smaller than 1.

Therefore, the RC design challenge can also be viewed as the selection of $L(z)$. The learning function $L(z)$ determines the RC system's transient response and the stability of the closed-loop system. A popular zero-phase learning function has been proposed in [87]. For stable minimum phase plant, the learning function is simply the inverse of $P(z)$ in (2), $L(z) = 1/P(z)$, as its inverse will have stable poles. Some other learning function designs can also be found in [86], [88]. Phase lead-based learning function has been proposed in [88]. Meanwhile, the work [86] introduces IIR filter-based learning functions. The design of learning function $L(z)$ depends on several factors such as (a) the accurate plant model is known or not, (b) the plant model is minimum or non-minimum phase, (c) the input delay and relative degree of plant model.

In this work, two types of learning functions offering less design complexities are considered, namely: proportional learning function $L_p(z)$ and zero-phase learning function $L_{zp}(z)$. The learning function $L_p(z)$ formulated by

$$L(z) = \gamma z^m, \tag{25}$$

where γ is a proportional gain and m is a relative degree of plant model given in (2). This learning function can be considered a straightforward design in the RC-controlled system. This is the case because the method only chooses the proportional gain γ and integer m, disregarding detail knowledge regarding the plant model. It is important to note that the gain γ can be adjusted to allow for a faster convergence rate of the tracking error. However, in order to maintain stability, the left-hand side value of (22) must remain less than one, as specified by the stability condition (22).

This study also employs the zero-phase learning function, in addition to the proportional-based learning function. The zero-phase learning function $L_{zp}(z)$ has the following expression:

$$L_{zp}(z) = P^{-1}(z), \tag{26}$$

where $P^{-1}(z)$ denotes the inverse model of (2). The term zero-phase implies that $L_{zp}(z)$ offers perfect phase compensation to the plant model $P(z)$. Thus,

$$\theta_{[L_{zp}(z)P(z)]}(\omega) = 0,\ 0 < \omega < {}^{\pi}/_{T}, \tag{27}$$

where $\theta_{[L_{zp}(z)P(z)]}(\omega)$ corresponds to the phase of transfer function $[L_{zp}(z)P(z)]$ at frequency ω.

In the next section, we provide simulation results of learning algorithms applied to Functional Electrical Stimulation (FES) based on closed-loop system illustrated in Fig. 3. Here, we analyze two distinct varieties of learning functions, namely the zero-phase learning function (Type B) and the proportional learning function (Type A), using the simulation results. In light of the practical implementations, the computational complexities associated with the control algorithms should not be an issue. This can be explained by Fig. 1 and Fig. 2, which show that ILC and RC are basically delayed-based control schemes. One-period delay/memory is utilized in the implementation of both ILC and RC, which is still practical in real-time implementation.

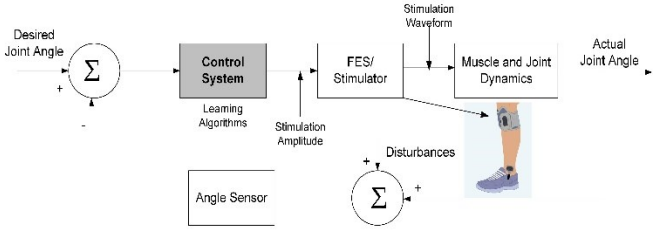

Fig. 3. Block diagram of closed-loop FES system with learning algorithms

In this work, we focus more on the analysis of the FES system comprising tracking accuracy, convergence rate, and the performance under model inaccuracies. We also use an assumption that measurement disturbances are not involved in this study. Then, a summary of the research methodology utilized in this study is provided in the flowchart depicted in Fig. 4.

Lastly, it is worth noting that certain investigations with alternative control methods, such as PID and SMC, are omitted here since they have already been addressed in some works [89] and [90]. These comparisons highlight the superior performance of ILC and RC algorithms, particularly in terms of tracking iterative trajectory. However, given that the trajectory is non-periodic, such as a unit step, the performance of the ILC/RC is inferior compared to even a PID-based controller.

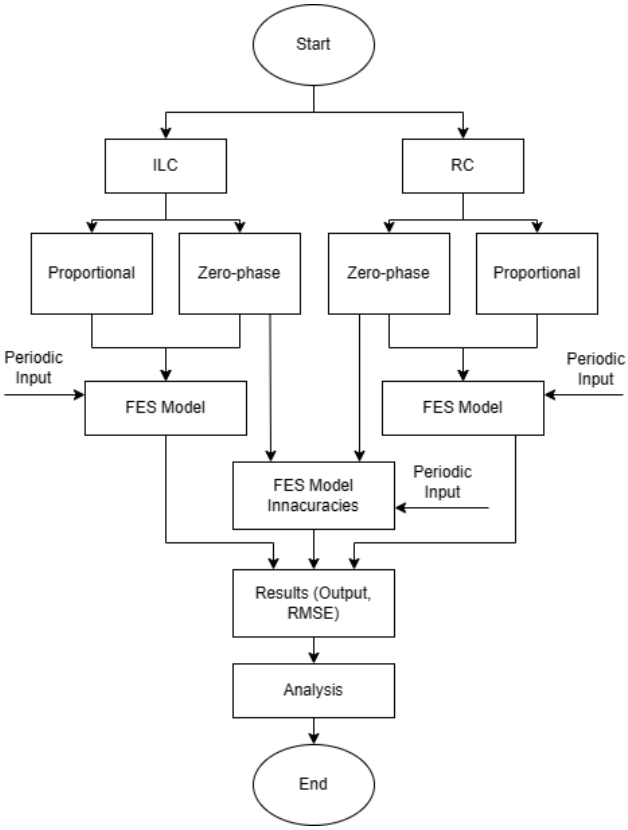

Fig. 4. A flowchart of the research methodology

III. RESULTS AND DISCUSSION

Let the following FES model is used in the simulation [91].

$$y(k) = \frac{b_2 z^{-2}}{1 + a_0 z^{-1} + a_1 z^{-2}} u(k) \tag{28}$$

where $a_0 = -0.8097$, $a_1 = -0.0777$, $b_2 = 0.6634$. The stimulation intensity which is the pulse widths in tenths milliseconds becomes the control input $u(k)$. The plant output $y(k)$ is an ankle joint angle in degrees. Table I is given to list the parameters required in the design of ILC and RC algorithms.

TABLE I. LIST OF REQUIRED PARAMETERS

Parameter	Value
Sampling time (T)	0.02 s
Period per iteration (T_r)	1 s
Number of samples per iteration (N)	50
Plant relative degree (m)	2
Plant parameters	a_0, a_1, b_2 (see 28)

In the simulation, the desired trajectory is an ankle joint angle as shown in Fig. 5 [91]. It is shown that the desired ankle angle ranges from -15^o to $+2^o$ for each iteration. Then, we aim to design ILC and RC algorithms such that the output $y(k)$ precisely follow the desired ankle angle.

The following subsection then presents the discussion of the ILC design setup, the simulation findings and analysis of the ILC-controlled FES system.

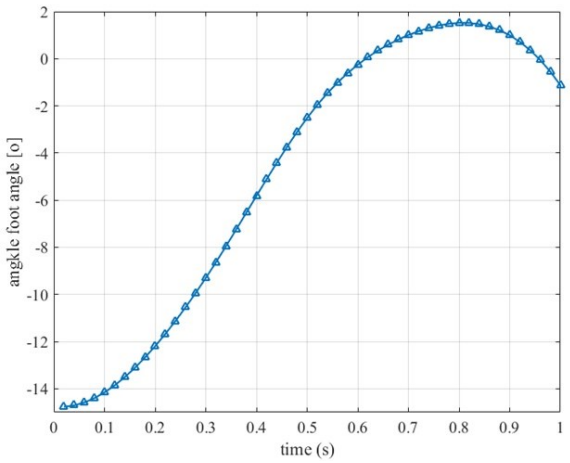

Fig. 5. Desired ankle joint angle per iteration

A. ILC Design Setup, Results, and Analysis

Based on (4), the state-space model of the given transfer function (28) has the following matrices:

$$A = \begin{bmatrix} 0.8097 & 0.0777 \\ 1 & 0 \end{bmatrix}, B = \begin{bmatrix} 1 \\ 0 \end{bmatrix}, \\ C = [0 \quad 0.6634], D = 0 \tag{29}$$

We begin with simplest design of ILC which is an ILC with proportional learning function L_p. The learning function L_p will be a diagonal matrix with diagonal values as γ. Variable γ is a gain in which we can adjust its value.

$$L_p = \begin{bmatrix} \gamma & 0 & \cdots & 0 \\ 0 & \gamma & 0 & 0 \\ \vdots & 0 & \ddots & 0 \\ 0 & \cdots & 0 & \gamma \end{bmatrix}, L_p \in \mathbb{R}^{50x50} \tag{30}$$

Let also choose small γ to start $\gamma = 0.1$. Applying control law (8) to the plant (28), we obtain simulation results as shown in Fig. 6 to Fig. 7. The evolution of plant output $y(k)$ can be seen in Fig. 6, while the root-means-square errors (RMSEs) for different values of γ can be found in Fig. 7.

We can see from Fig. 6 that the plant output is zero during the first iteration. This is due to zero control signal during the

first iteration. Fig. 6 also indicates that the plant output moves to follow the reference signal as the iteration increases.

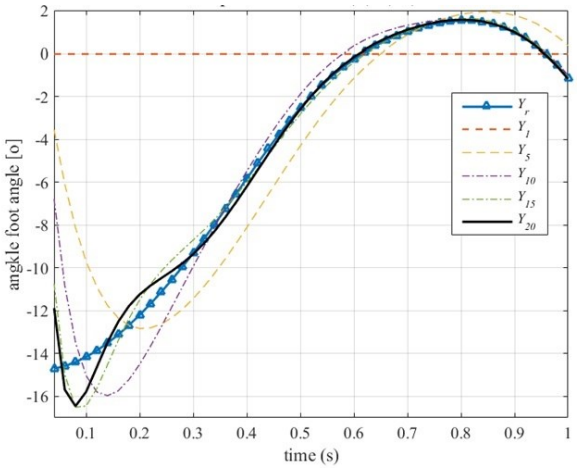

Fig. 6. ILC tracking output evolution at iteration $j = 1; 5; 10; 20; 25$

The convergence rate of ILC system with gain 0.1 is very slow as indicated in Fig. 7. The RMS error reaches zero after about 90 iterations. Fig. 7 also indicates that increasing the gain of proportional learning function to a certain degree will faster the convergence rate. We simulate that increasing the gain larger than 0.3 ends up to unstable system. The unstable system means that when we apply $\gamma > 0.3$, the RMSE tends to diverge as the iteration increases. This implies that the stability condition given in (17) is violated.

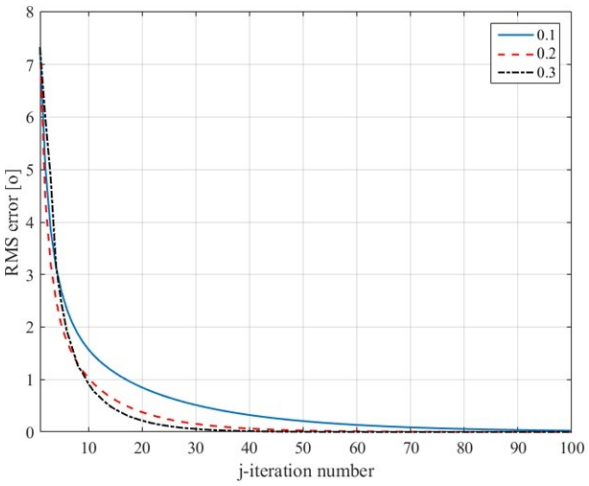

Fig. 7. RMS error evolution of ILC at three different gains

Now, we examine the performance of ILC system when a zero-phase learning matrix L_{zp} is employed. The following learning matrix is applied:

$$L_{zp} = \begin{bmatrix} 1.50 & 0 & 0 & \cdots & 0 \\ -1.22 & 1.50 & 0 & \cdots & 0 \\ -0.11 & -1.22 & \ddots & 0 & \vdots \\ 0 & \ddots & \ddots & 1.50 & 0 \\ 0 & 0 & -0.11 & -1.22 & 1.50 \end{bmatrix}, L_{zp} \in \mathbb{R}^{50x50} \quad (31)$$

Note that the above learning matrix is computed based on (16). Fig. 8 indicates that the plant output can perfectly follow the trajectory after one iteration.

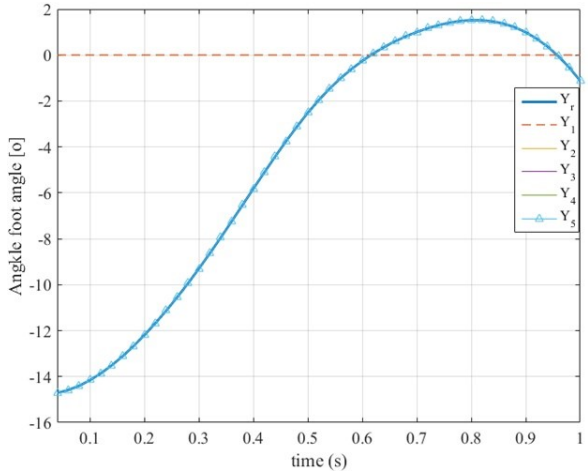

Fig. 8. Plant output evolution of ILC with zero-phase learning function

This can also be seen from Fig. 9, where the RMSE reached zero after one iteration. We can notice the differences in performance between ILC system with proportional learning function and ILC system with zero phase learning function. Now, we test the performance of ILC with zero phase learning function when there are model inaccuracies. Suppose 10 percent variations vary the plant parameters in (28). Then we get $a_0 = -0.7287, a_2 = -0.0699, b_2 = 0.5971$.

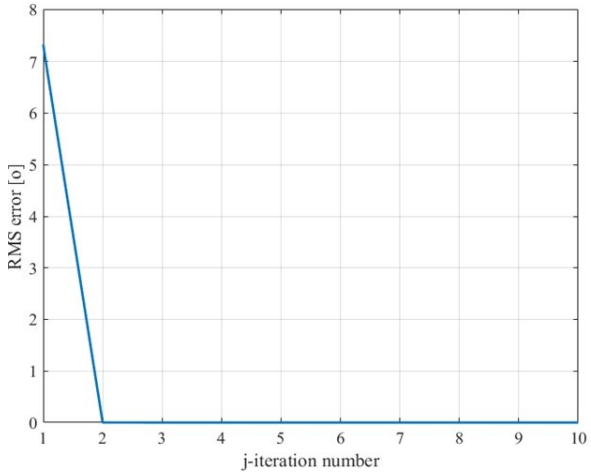

Fig. 9. ILC RMS error with zero-phase learning function

The tracking performance of ILC with zero-phase learning function under plant parameters variation is shown in Fig. 10 and Fig. 11. We notice that an inaccurate model results in slower convergence for ILC with zero-phase learning function. The slower convergence here means that the patient requires more time or longer iterations until his or her ankle joint can perfectly follow the desired trajectory.

The ILC system with proportional learning function has a simpler design because it does not require complete plant model information. In this type of ILC system, the design objective is to select the gain for give faster convergence rate while keeping the system stable. According to [92], the gain γ should be chosen to satisfy the condition (32). The condition (32) shows that the choice of γ uses the information of input and matrices B and C, but it does not require the information of system matrix A.

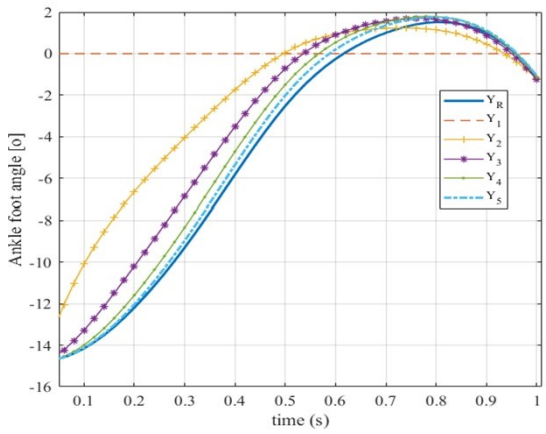

Fig. 10. Tracking performance of ILC under model inaccuracies plant output evolution with zero-phase learning function

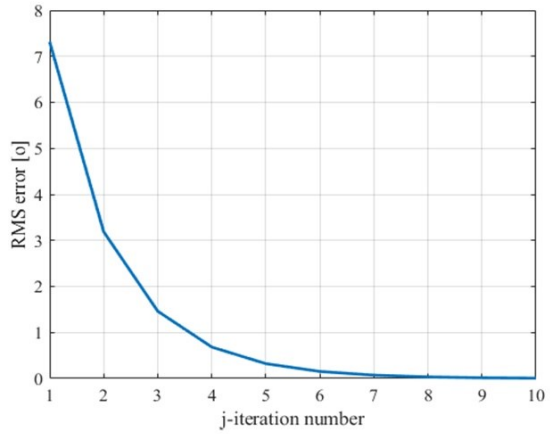

Fig. 11. Tracking performance of ILC under model inaccuracies RMS error zero-phase learning function

$$0 < CB\gamma < 2 \tag{32}$$

In other words, the design technique does not require all of the plant model's information (28). The ILC system with zero-phase learning function, on the other hand, necessitates an accurate plant model in the design. Furthermore, using an inaccurate plant model in the design of an ILC system with a zero-phase learning function leads to slower error convergence. Following the ILC design and results, the subsequent subsection proceeds with the RC design configuration and an analysis of the simulation results for the FES system that is controlled by the RC.

B. RC Design Setup, Results, and Analysis

In this part, we begin by examining the performance of RC with proportional lead learning function. The following RC control law is applied to the plant (28)

$$u(k) = u(k-50) + \gamma z^m e(k-50) \tag{33}$$

Variable γ is proportional gain, while m is lead step picked from the relative degree of the plant (28). The tracking performance of RC system with learning function $[0.1z^2]$ can be seen in Fig. 12 and Fig. 13. Fig. 12 shows the tracking output for the first 10 iterations. We notice zero tracking output during the first iteration, then the tracking output moves to follow the reference as the iteration increases. The RC's RMSE at three different gains can be seen in Fig. 13. As we increase the gain from 0.1 to 0.2, the convergence rate gets faster, and the RMSE asymptotically decreases. This indicates that the tracking output requires fewer iterations to precisely follow the intended trajectory at gain 0.2 compared to gain 0.1. At gain 0.3, we see that the convergence rate is not improving compared to the gain 0.2. Moreover, the RMSE does not smoothly decrease. This behavior does not guarantee the long-term stability at this gain value.

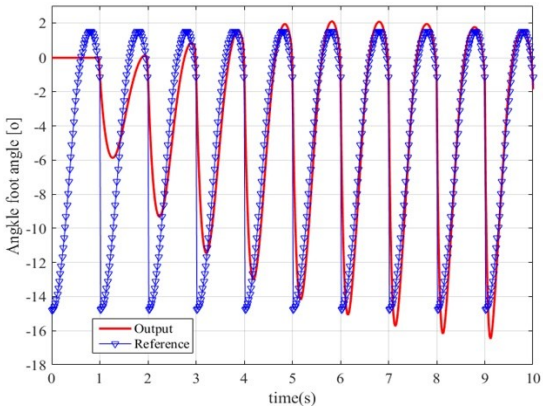

Fig. 12. RC plant output evolution with learning function $L(z) = 0.1z^2$

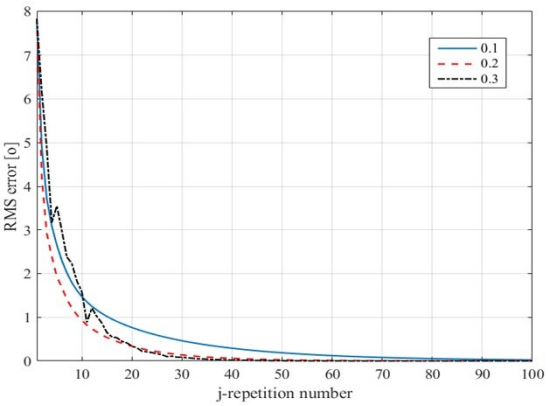

Fig. 13. RMSE of RC system with proportional learning function at three different gains

We also examine the performance of RC when zero-phase learning function is used. The following RC control law is applied:

$$u(k) = u(k-50) + L_{zp}(z)e(k-50), \tag{34}$$

where $L_{zp}(z)$ is given as

$$L_{zp}(z) = 1.507z^2 - 1.220z - 0.117\,. \tag{35}$$

The tracking performance of RC system with zero-phase learning function can be seen in Fig. 14 to Fig. 17. Fig. 14 shows that the RC output perfectly follows the desired trajectory after one iteration, while Fig. 15 shows RMSE confirming that the tracking error of the zero-phase learning function significantly out-performed the proportional learning function in the term the convergence rate. This behavior indicates that two iterations are necessary for the patient's ankle joint to precisely track the intended trajectory. The performance of RC with zero phase learning function is also tested for model inaccuracies.

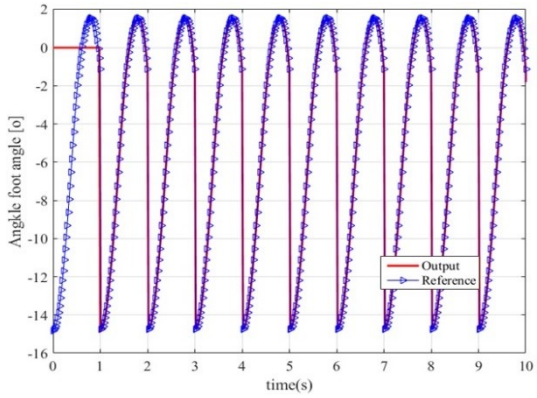

Fig. 14. RC plant output evolution with zero-phase learning function

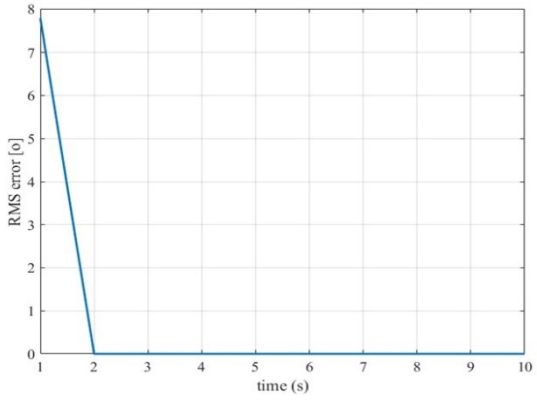

Fig. 15. RC RMSE with zero-phase learning function

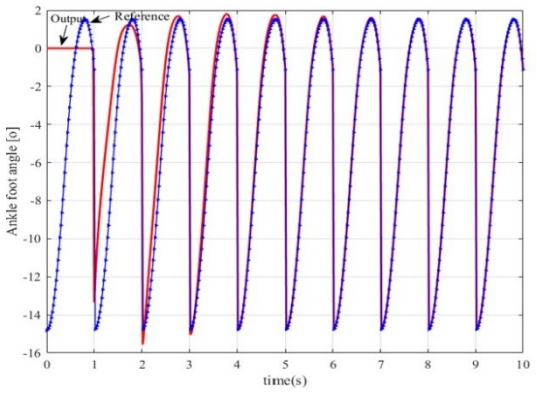

Fig. 16. Tracking performance of RC under model inaccuracies plant output evolution with zero-phase learning function

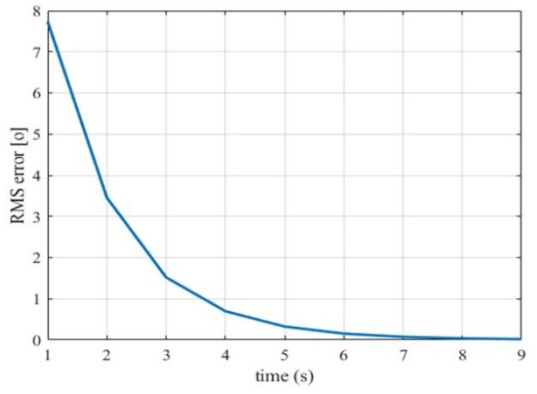

Fig. 17. Tracking performance of RC under model inaccuracies RMS error with zero-phase learning function

The results are shown in Fig. 16 and Fig. 17, where we can see similar results to ILC's. These confirm that the zero-phase learning function's performance depends on how accurate the plant model is known. To cope with this issue, RC could be employed in tandem with other control schemes such as observer-based, robust, and adaptive control approaches.

Based on the results shown in Fig. 6 to Fig. 17, it can be concluded that accurate tracking shown by a zero-tracking error is realizable for both ILC and RC methods given that the trajectory is iterative. It can also be noted that the zero-phase learning function provides faster convergence compared to the proportional learning function. However, the proportional learning function is simpler in design as it does not need a complete plant model. Finally, it is also noticeable that the model inaccuracies affect the convergence rate of the controlled system.

IV. CONCLUSION

This article has presented a simulation study of repetitive control (RC) and iterative learning control (ILC) for controlling FES with iterative trajectory. The important results are that an accurate tracking given by a zero-tracking error are realizable for both ILC and RC methods. Several ILC and RC designs for two different learning functions, namely proportional and zero-phase learning functions, are given. The proportional learning function has simpler design as it does not need the plant model. This is further supported by the formula of the learning function, which requires only the gain value. The concern is about tuning the gain to give faster convergence rate, while ensuring long-term stability. While increasing the proportional gain can accelerate convergence, doing so to an excessive degree can lead to system instability. The precise plant model is a prerequisite for the zero-phase learning function, which can be further clarified using the formula for the learning function. Given the accurate plant model, the convergence of zero-phase learning systems can be guaranteed within 2 iterations. This suggests that two iterations are necessary for the zero-phase learning function to guarantee that the ankle angle of the patient precisely follows the desired trajectory. However, the convergence rate of zero-phase learning systems is decreased when the plant model is accurate. Both ILC and RC systems work properly when the plant model is accurately known, and the trajectory period is perfectly constant.

In practical applications, the trajectory period may be uncertain, or the period may slightly change for each iteration. In addition, the plant model can be partially known or completely unknown. These conditions can make the tracking performance degrade. Therefore, ILC and RC designs for classes of unknown plant model with uncertain reference period are very challenging which can become potential future research works. ILC and RC can be utilized in conjunction with other control schemes, such as observer-based, robust, and adaptive control schemes, to address these research challenges. In conclusion, the study indicates that there is hardly a noticeable performance difference between ILC and RC systems. This indicates that both ILC and RC have significant potential as control methods for FES,

particularly when the control goal is for tracking iterative trajectories.

ACKNOWLEDGMENT

The authors would like to thank the Research Center for Photonics and Research Organization of Nanotechnology and Materials, National Research and Innovation Agency (BRIN) for supporting this research work under research cluster Fundamental Sciences.

REFERENCES

[1] N. A. Alawad, A. J. Humaidi, A. S. M. Al-Obaidi, and A. S. Alaraji, "Active Disturbance Rejection Control of Wearable Lower-Limb System Based on Reduced ESO," *Indones. J. Sci. Technol.*, vol. 7, no. 2, pp. 203–218, 2022, doi: 10.17509/ijost.v7i2.46435.

[2] C.-F. Chen *et al.*, "Development and Hybrid Control of an Electrically Actuated Lower Limb Exoskeleton for Motion Assistance," *IEEE Access*, vol. 7, pp. 169107–169122, 2019, doi: 10.1109/ACCESS.2019.2953302.

[3] S. A. Moezi, R. Sedaghati, and S. Rakheja, "Nonlinear dynamic modeling and model-based AI-driven control of a magnetoactive soft continuum robot in a fluidic environment," *ISA Trans.*, 2023, doi: 10.1016/j.isatra.2023.10.030.

[4] L. Zhao, X. Liu, and T. Wang, "Trajectory tracking control for double-joint manipulator systems driven by pneumatic artificial muscles based on a nonlinear extended state observer," *Mech. Syst. Signal Process.*, vol. 122, pp. 307–320, 2019, doi: 10.1016/j.ymssp.2018.12.016.

[5] L. Zhao, X. Liu, J. Zhang, and T. Wang, "Angle tracking control for double-joint dexterous hand systems based on a piecewise extended state observer," *Control Eng. Pract.*, vol. 110, p. 104754, 2021, doi: 10.1016/j.conengprac.2021.104754.

[6] Q. Yang, W. Wang, Y. Zhang, Q. Yan, and J. Cai, "Angle Error-Tracking Iterative Learning Control for Pneumatic Artificial Muscle System," *IEEE Access*, vol. 9, pp. 163099–163107, 2021, doi: 10.1109/ACCESS.2021.3133864.

[7] Y. Yu and S. Lai, "Initial-Rectification Barrier Iterative Learning Control for Pneumatic Artificial Muscle Systems With Nonzero Initial Errors and Iteration-Varying Reference Trajectories," *IEEE Access*, vol. 10, pp. 24194–24202, 2022, doi: 10.1109/ACCESS.2022.3155694.

[8] R. Wu, Z. Yao, J. Si, and H. H. Huang, "Robotic Knee Tracking Control to Mimic the Intact Human Knee Profile Based on Actor-Critic Reinforcement Learning," *IEEE/CAA J. Autom. Sin.*, vol. 9, no. 1, pp. 19–30, 2022, doi: 10.1109/JAS.2021.1004272.

[9] E. Al Khatib, P. Razzaghi, and Y. Hurmuzlu, "Feedback control of millimeter scale pivot walkers using magnetic actuation," *Rob. Auton. Syst.*, vol. 168, p. 104496, 2023, doi: 10.1016/j.robot.2023.104496.

[10] V. Chertopolokhov, O. Andrianova, A. Hernandez-Sanchez, C. Mireles, A. Poznyak, and I. Chairez, "Averaged sub-gradient integral sliding mode control design for cueing end-effector acceleration of a two-link robotic arm," *ISA Trans.*, vol. 133, pp. 134–146, 2023, doi: 10.1016/j.isatra.2022.07.024.

[11] R. Padmanabhan, N. Meskin, C. M. Ionescu, and W. M. Haddad, "A nonovershooting tracking controller for simultaneous infusion of anesthetics and analgesics," *Biomed. Signal Process. Control*, vol. 49, pp. 375–387, 2019, doi: 10.1016/j.bspc.2018.09.015.

[12] J. Gastinger, D. Müller, A. Hildebrandt, and O. Sawodny, "Pose Estimation and Tracking Control of a Pneumatic Soft Robotic Hand," *IFAC-PapersOnLine*, vol. 53, no. 2, pp. 9962–9967, 2020, doi: 10.1016/j.ifacol.2020.12.2712.

[13] K. Ba *et al.*, "Dynamics compensation of impedance-based motion control for LHDS of legged robot," *Rob. Auton. Syst.*, vol. 139, p. 103704, 2021, doi: 10.1016/j.robot.2020.103704.

[14] V. Oguntosin and A. Abdulkareem, "Design of a pneumatic soft actuator controlled via eye tracking and detection," *Heliyon*, vol. 6, no. 7, p. e04388, 2020, doi: 10.1016/j.heliyon.2020.e04388.

[15] C. L. Lynch and M. R. Popovic, "Stimulation of Induced Muscle Contractions," *IEEE Control Syst. Mag.*, pp. 40–50, 2008.

[16] V. Ghanbari, V. H. Duenas, P. J. Antsaklis, and W. E. Dixon, "Passivity-Based Iterative Learning Control for Cycling Induced by Functional Electrical Stimulation With Electric Motor Assistance," *IEEE Trans. Control Syst. Technol.*, vol. 27, no. 5, pp. 2287–2294, 2019, doi: 10.1109/TCST.2018.2854773.

[17] E. Jafari and A. Erfanian, "A Distributed Automatic Control Framework for Simultaneous Control of Torque and Cadence in Functional Electrical Stimulation Cycling," *IEEE Trans. Neural Syst. Rehabil. Eng.*, vol. 30, pp. 1908–1919, 2022, doi: 10.1109/TNSRE.2022.3188735.

[18] B. C. Allen, K. J. Stubbs, and W. E. Dixon, "Robust cadence tracking for switched FES-cycling using a time-varying estimate of the electromechanical delay," *Automatica*, vol. 144, no. 2, pp. 827–834, 2022, doi: 10.1016/j.automatica.2022.110466.

[19] N. Hayami *et al.*, "Development and Validation of a Closed-Loop Functional Electrical Stimulation-Based Controller for Gait Rehabilitation Using a Finite State Machine Model," *IEEE Trans. Neural Syst. Rehabil. Eng.*, vol. 30, pp. 1642–1651, 2022, doi: 10.1109/TNSRE.2022.3183571.

[20] S. Akbari, G. Merritt, F. M. Zegers, and C. A. Cousin, "A Hybrid Systems Approach to Dual-Objective Functional Electrical Stimulation Cycling," *IEEE Control Syst. Lett.*, vol. 6, pp. 2126–2131, 2022, doi: 10.1109/LCSYS.2021.3138190.

[21] Y. Kushima, Y. Araki, H. Kawai, T. Murao, Y. Kawai, and M. Kishitani, "Velocity Tracking Control of Recumbent Trike with Functional Electrical Stimulation," *IFAC-PapersOnLine*, vol. 53, no. 5, pp. 207–211, 2020, doi: 10.1016/j.ifacol.2021.04.210.

[22] Z. Sun, X. Bao, Q. Zhang, K. Lambeth, and N. Sharma, "A Tube-based Model Predictive Control Method for Joint Angle Tracking with Functional Electrical Stimulation and An Electric Motor Assist," *Proc. Am. Control Conf.*, vol. 2021, no. 5, pp. 1390–1395, 2021, doi: 10.23919/ACC50511.2021.9483084.

[23] B. C. Allen, K. J. Stubbs, and W. E. Dixon, "Adaptive trajectory tracking during motorized and fes-induced biceps curls via integral concurrent learning," *ASME 2020 Dyn. Syst. Control Conf. DSCC 2020*, vol. 1, pp. 2557–2566, 2020, doi: 10.1115/DSCC2020-3125.

[24] Y. Hasegawa, T. Kitamura, S. Sakaino, and T. Tsuji, "Bilateral control of elbow and shoulder joints using functional electrical stimulation between humans and robots," *IEEE Access*, vol. 8, pp. 15792–15799, 2020, doi: 10.1109/ACCESS.2020.2967466.

[25] E. Kurniawan *et al.*, "Low-order sliding mode repetitive control for uncertain linear systems perturbed by band-limited periodic disturbances," *Proc. Inst. Mech. Eng. Part I J. Syst. Control Eng.*, vol 237, no 9, 2023, doi: 10.1177/09596518231165566.

[26] E. Kurniawan, H. Wang, B. H. Sirenden, J. A. Prakosa, H. Adinanta, and S. Suryadi, "Discrete-time modified repetitive sliding mode control for uncertain linear systems," *Int. J. Adapt. Control Signal Process.*, vol. 35, no. 11, pp. 2245–2258, 2021, doi: 10.1002/acs.3316.

[27] E. Kurniawan *et al.*, "Robust adaptive repetitive control for unknown linear systems with odd-harmonic periodic disturbances," *Sci. China Inf. Sci.*, vol. 65, no. 12, p. 222202, 2022, doi: 10.1007/s11432-022-3561-2.

[28] M. Mitrevska, Z. Cao, J. Zheng, E. Kurniawan, and Z. Man, "Discrete terminal sliding mode repetitive control for a linear actuator with nonlinear friction and uncertainties," *Int. J. Robust Nonlinear Control*, vol. 29, no. 13, pp. 4285–4297, 2019, doi: 10.1002/rnc.4639.

[29] E. Kurniawan *et al.*, "Variable-structure repetitive control for discrete-time linear systems with multiple-period exogenous signals," *Int. J. Appl. Math. Comput. Sci.*, vol. 30, no. 2, pp. 207–218, 2020, doi: 10.34768/amcs-2020-0016.

[30] S. Arimoto, S. Kawamura, and F. Miyazaki, "Bettering operation of Robots by learning," *J. Robot. Syst.*, vol. 1, no. 2, pp. 123–140, 1984, doi: 10.1002/rob.4620010203.

[31] Y. Chen, D. Huang, Y. Li, and X. Feng, "A Novel Iterative Learning Approach for Tracking Control of High-Speed Trains Subject to Unknown Time-Varying Delay," *IEEE Trans. Autom. Sci. Eng.*, vol. 19, no. 1, pp. 113–121, 2022, doi: 10.1109/TASE.2020.3041952.

[32] Q. Yu and Z. Hou, "Adaptive Fuzzy Iterative Learning Control for High-Speed Trains with Both Randomly Varying Operation Lengths and System Constraints," *IEEE Trans. Fuzzy Syst.*, vol. 29, no. 8, pp. 2408–2418, 2021, doi: 10.1109/TFUZZ.2020.2999958.

[33] D. Huang, Y. Chen, D. Meng and P. Sun, "Adaptive Iterative Learning Control for High-Speed Train: A Multi-Agent Approach," in *IEEE Transactions on Systems, Man, and Cybernetics: Systems*, vol. 51, no. 7, pp. 4067-4077, 2021.

[34] I. Trojaola, I. Elorza, E. Irigoyen, A. Pujana-Arrese, and C. Calleja, "Iterative learning control and Gaussian process regression for hydraulic cushion control," *IFAC-PapersOnLine*, vol. 53, no. 2, pp. 1421–1426, 2020, doi: 10.1016/j.ifacol.2020.12.1909.

[35] Q. Li, Z. Ruan, L. Guo, and C. Ding, "Clamp-shear coupling compensation of a walking piezo actuator combining ILC and hysteresis compensation," *Mech. Syst. Signal Process.*, vol. 208, p. 110964, 2024, doi: 10.1016/j.ymssp.2023.110964.

[36] R. Wang, Z. Zhuang, H. Tao, W. Paszke, and V. Stojanovic, "Q-learning based fault estimation and fault tolerant iterative learning control for MIMO systems," *ISA Trans.*, vol. 142, pp. 123–135, 2023, doi: 10.1016/j.isatra.2023.07.043.

[37] F. Browne, B. Rees, G. T. C. Chiu, and N. Jain, "Iterative Learning Control with Time-Delay Compensation: An Application to Twin-Roll Strip Casting," *IEEE Trans. Control Syst. Technol.*, vol. 29, no. 1, pp. 140–149, 2021, doi: 10.1109/TCST.2020.2971452.

[38] L. Hladowski, K. Galkowski, and E. Rogers, "Practical Application of the Dynamic Output-Only Iterative Learning Control Design To The Crane System*," *IFAC-PapersOnLine*, vol. 55, no. 12, pp. 476–481, 2022, doi: 10.1016/j.ifacol.2022.07.357.

[39] Z. Shahriari, G. A. Dumont, and K. Fong, "Iterative Learning Control for Beam Loading Cancellation in Electron Linear Accelerator," *IFAC-PapersOnLine*, vol. 54, no. 21, pp. 55–60, 2021, doi: 10.1016/j.ifacol.2021.12.010.

[40] Z. Hong, Q. Yan, X. Wu, and J. Cai, "Fuzzy System-Based Position Tracking Iterative Learning Control for Tank Gun Control Systems with Error Constraints," *IEEE Access*, vol. 10, pp. 52462–52471, 2022, doi: 10.1109/ACCESS.2022.3175838.

[41] J. C. Ren, D. Liu, and Y. Wan, "Model-Free Adaptive Iterative Learning Control Method for the Czochralski Silicon Monocrystalline Batch Process," *IEEE Trans. Semicond. Manuf.*, vol. 34, no. 3, pp. 398–407, 2021, doi: 10.1109/TSM.2021.3074625.

[42] H. Xie, Y. Wen, X. Shen, H. Zhang, and L. Sun, "High-Speed AFM Imaging of Nanopositioning Stages Using H∞ and Iterative Learning Control," *IEEE Trans. Ind. Electron.*, vol. 67, no. 3, pp. 2430–2439, 2020, doi: 10.1109/TIE.2019.2902792.

[43] L. Bingqiang, L. Tianyi, Z. Yiyun, and L. Shuaishuai, "Open-loop and closed-loop Dα-type iterative learning control for fractional-order linear multi-agent systems with state-delays," *J. Syst. Eng. Electron.*, vol. 32, no. 1, pp. 197–208, 2021, doi: 10.23919/JSEE.2021.000017.

[44] D. X. Ba, N. T. Thien, and J. Bae, "A Novel Iterative Second-Order Neural-Network Learning Control Approach for Robotic Manipulators," *IEEE Access*, vol. 11, pp. 58318–58332, 2023, doi: 10.1109/ACCESS.2023.3280979.

[45] J. Dong, B. He, M. Ming, C. Zhang, and G. Li, "Design of Open-Closed-Loop Iterative Learning Control With Variable Stiffness for Multiple Flexible Manipulator Robot Systems," *IEEE Access*, vol. 7, pp. 23163–23168, 2019, doi: 10.1109/ACCESS.2019.2898266.

[46] C. E. Boudjedir, M. Bouri, and D. Boukhetala, "Model-Free Iterative Learning Control With Nonrepetitive Trajectories for Second-Order MIMO Nonlinear Systems—Application to a Delta Robot," *IEEE Trans. Ind. Electron.*, vol. 68, no. 8, pp. 7433–7443, 2021, doi: 10.1109/TIE.2020.3007091.

[47] L. Yang, Y. Li, D. Huang, J. Xia, and X. Zhou, "Spatial Iterative Learning Control for Robotic Path Learning," *IEEE Trans. Cybern.*, vol. 52, no. 7, pp. 5789–5798, 2022, doi: 10.1109/TCYB.2021.3138992.

[48] H. Fu, C. Hu, D. Yu, Y. Zhu, and M. Zhang, "Cascaded iterative learning motion control of precision maglev planar motor with experimental investigation," *ISA Trans.*, vol. 139, pp. 463–474, 2023, doi: 10.1016/j.isatra.2023.03.031.

[49] D. Meng, "Convergence Conditions for Solving Robust Iterative Learning Control Problems Under Nonrepetitive Model Uncertainties," *IEEE Trans. Neural Networks Learn. Syst.*, vol. 30, no. 6, pp. 1908–1919, 2019, doi: 10.1109/TNNLS.2018.2874977.

[50] T. Zhang, X. Jiao, and Y. Zhang, "Internal-Model-Principle-Based Fast Adaptive Iterative Learning Trajectory Tracking Control for Autonomous Farming Vehicle Under Alignment Condition and Input Constraint," *IEEE Trans. Syst. Man, Cybern. Syst.*, vol. 53, no. 6, pp. 3588–3599, 2023, doi: 10.1109/TSMC.2022.3229523.

[51] Q. Shi, X. Huang, B. Meng, and Z. Wang, "Neural network-based iterative learning control for trajectory tracking of unknown SISO nonlinear systems," *Expert Syst. Appl.*, vol. 232, p. 120863, 2023, doi: 10.1016/j.eswa.2023.120863.

[52] Z. Afkhami, D. J. Hoelzle, and K. Barton, "Robust Higher-Order Spatial Iterative Learning Control for Additive Manufacturing Systems," *IEEE Trans. Control Syst. Technol.*, vol. 31, no. 4, pp. 1692–1707, 2023, doi: 10.1109/TCST.2023.3243397.

[53] M. Cobb, J. Reed, M. Wu, K. D. Mishra, K. Barton, and C. Vermillion, "Flexible-Time Receding Horizon Iterative Learning Control With Application to Marine Hydrokinetic Energy Systems," *IEEE Trans. Control Syst. Technol.*, vol. 30, no. 6, pp. 2767–2774, 2022, doi: 10.1109/TCST.2022.3165734.

[54] K. L. Moore, Y. Chen, and H.-S. Ahn, "Iterative Learning Control: A Tutorial and Big Picture View," in *Proceedings of the 45th IEEE Conference on Decision and Control*, pp. 2352–2357, 2006. doi: 10.1109/CDC.2006.377582.

[55] D. A. Bristow, M. Tharayil, and A. G. Alleyne, "A survey of iterative learning control," *IEEE Control Syst. Mag.*, vol. 26, no. 3, pp. 96–114, 2006, doi: 10.1109/MCS.2006.1636313.

[56] Y. Yang, X. Dong, X. Liu, and D. Huang, "Robust Repetitive Learning-Based Trajectory Tracking Control for a Leg Exoskeleton Driven by Hybrid Hydraulic System," *IEEE Access*, vol. 8, pp. 27705–27714, 2020, doi: 10.1109/ACCESS.2020.2971777.

[57] A. Tilli, E. Ruggiano, C. Conficoni, and A. Bosso, "A Hybrid Adaptation Strategy for Repetitive Control of an Uncertain-Delay Lagrangian System," *IFAC-PapersOnLine*, vol. 53, no. 2, pp. 8965–8972, 2020, doi: 10.1016/j.ifacol.2020.12.1483.

[58] L. Blanken, P. Bevers, S. Koekebakker, and T. Oomen, "Sequential Multiperiod Repetitive Control Design With Application to Industrial Wide-Format Printing," *IEEE/ASME Trans. Mechatronics*, vol. 25, no. 2, pp. 770–778, 2020, doi: 10.1109/TMECH.2020.2967305.

[59] Y. Cao and Z. Zhang, "Cross-Coupled Repetitive Control of a Compliant Nanomanipulator for Micro-Stereolithography," *IEEE Access*, vol. 8, pp. 3891–3900, 2020, doi: 10.1109/ACCESS.2019.2962967.

[60] P. Cui, H. Xu, Z. Liu, J. Li, and B. Han, "Improved Second-Order Repetitive Control With Parameter Optimization for Magnetically Suspended Rotor System," *IEEE Sens. J.*, vol. 20, no. 5, pp. 2294–2303, 2020, doi: 10.1109/JSEN.2019.2951764.

[61] P. Cui, Q. Wang, G. Zhang, and Q. Gao, "Hybrid Fractional Repetitive Control for Magnetically Suspended Rotor Systems," *IEEE Trans. Ind. Electron.*, vol. 65, no. 4, pp. 3491–3498, 2018, doi: 10.1109/TIE.2017.2752119.

[62] P. Cui, H. Xu, Z. Liu, B. Han, and H. Li, "Harmonic Current Suppression of Magnetically Suspended Rotor System via Odd-Harmonic Fractional RC," *IEEE Sens. J.*, vol. 19, no. 13, pp. 4812–4819, 2019, doi: 10.1109/JSEN.2019.2901937.

[63] M. Mitrevska, Z. Cao, J. Zheng, E. Kurniawan, and Z. Man, "Design of a Robust Discrete-time Phase Lead Repetitive Control in Frequency Domain for a Linear Actuator with Multiple Phase Uncertainties," *Int. J. Control. Autom. Syst.*, vol. 16, no. 6, pp. 2609–2620, 2018, doi: 10.1007/s12555-017-0208-x.

[64] Z. Zhang, B. Chu, Y. Liu, H. Ren, Z. Li, and D. H. Owens, "Multiperiodic Repetitive Control for Functional Electrical Stimulation-Based Wrist Tremor Suppression," *IEEE Trans. Control Syst. Technol.*, vol. 30, no. 4, pp. 1494–1509, 2022, doi: 10.1109/TCST.2021.3111107.

[65] Z. Zhang, B. Chu, Y. Liu, Z. Li, and D. H. Owens, "Multimuscle Functional-Electrical-Stimulation-Based Wrist Tremor Suppression Using Repetitive Control," *IEEE/ASME Trans. Mechatronics*, pp. 1–11, 2022, doi: 10.1109/TMECH.2022.3150301.

[66] A. Lunardi, E. Conde, J. Assis, L. Meegahapola, D. A. Fernandes, and A. J. S. Filho, "Repetitive Predictive Control for Current Control of Grid-Connected Inverter Under Distorted Voltage Conditions," *IEEE Access*, vol. 10, pp. 16931–16941, 2022, doi: 10.1109/ACCESS.2022.3147812.

[67] Q. Zhao, H. Zhang, Y. Gao, S. Chen, and Y. Wang, "Novel Fractional-Order Repetitive Controller Based on Thiran IIR Filter for Grid-Connected Inverters," *IEEE Access*, vol. 10, pp. 82015–82024, 2022, doi: 10.1109/ACCESS.2022.3196776.

[68] J. Ye, L. Liu, J. Xu, and A. Shen, "Frequency Adaptive Proportional-Repetitive Control for Grid-Connected Inverters," *IEEE Trans. Ind. Electron.*, vol. 68, no. 9, pp. 7965–7974, 2021, doi: 10.1109/TIE.2020.3016247.

[69] T. Chmielewski, W. Jarzyna, D. Zieliński, K. Gopakumar, and M.

Chmielewska, "Modified repetitive control based on comb filters for harmonics control in grid-connected applications," *Electr. Power Syst. Res.*, vol. 200, p. 107412, 2021, doi: 10.1016/j.epsr.2021.107412.

[70] A. Straś, B. Ufnalski, M. Michalczuk, A. Gałecki, and L. Grzesiak, "Design of fractional delay repetitive control with a dead-beat compensator for a grid-tied converter under distorted grid voltage conditions," *Control Eng. Pract.*, vol. 98, p. 104374, 2020, doi: 10.1016/j.conengprac.2020.104374.

[71] T. Ohashi, H. Shibata, S. Futami, and R. Sato, "Nanometer-Order Contouring Control in a Feed Drive System Using Linear Ball Guides by Applying a Combination of Modified Disturbance Observer and Repetitive Control," *Nanomanufacturing Metrol.*, vol. 4, no. 2, pp. 118–129, 2021, doi: 10.1007/s41871-020-00095-y.

[72] L.-W. Shih and C.-W. Chen, "Model-free repetitive control design and implementation for dynamical galvanometer-based raster scanning," *Control Eng. Pract.*, vol. 122, p. 105124, 2022, doi: 10.1016/j.conengprac.2022.105124.

[73] L. Li, A. J. Fleming, Y. K. Yong, S. S. Aphale, and L. Zhu, "High performance raster scanning of atomic force microscopy using Model-free Repetitive Control," *Mech. Syst. Signal Process.*, vol. 173, p. 109027, 2022, doi: 10.1016/j.ymssp.2022.109027.

[74] J. Reinders, M. Giaccagli, B. Hunnekens, D. Astolfi, T. Oomen, and N. van de Wouw, "Repetitive Control for Lur'e-Type Systems: Application to Mechanical Ventilation," *IEEE Trans. Control Syst. Technol.*, vol. 31, no. 4, pp. 1819–1829, 2023, doi: 10.1109/TCST.2023.3250966.

[75] S. Tian, K.-Z. Liu, M. Zhang, C. Lu, M. Wu, and J. She, "Harmonic Disturbance Suppression for High-Performance Nonlinear Repetitive-Control Systems," *IFAC-PapersOnLine*, vol. 56, no. 2, pp. 4545–4550, 2023, doi: 10.1016/j.ifacol.2023.10.952.

[76] Y.-H. Lan, J.-L. He, P. Li, and J.-H. She, "Optimal preview repetitive control with application to permanent magnet synchronous motor drive system," *J. Franklin Inst.*, vol. 357, no. 15, pp. 10194–10210, 2020, doi: 10.1016/j.jfranklin.2020.04.026.

[77] Q. Chen, X. Yu, M. Sun, C. Wu, and Z. Fu, "Adaptive Repetitive Learning Control of PMSM Servo Systems with Bounded Nonparametric Uncertainties: Theory and Experiments," *IEEE Trans. Ind. Electron.*, vol. 68, no. 9, pp. 8626–8635, 2021, doi: 10.1109/TIE.2020.3016257.

[78] R. Chuei and Z. Cao, "Extreme learning machine-based super-twisting repetitive control for aperiodic disturbance, parameter uncertainty, friction, and backlash compensations of a brushless DC servo motor," *Neural Comput. Appl.*, vol. 32, no. 18, pp. 14483–14495, 2020, doi: 10.1007/s00521-020-04965-w.

[79] A. K. Seth and M. Singh, "Modified repetitive control design for two stage off board Electric Vehicle charger," *ISA Trans.*, vol. 128, pp. 343–356, 2022, doi: 10.1016/j.isatra.2021.09.015.

[80] Z. Feng, M. Ming, J. Ling, X. Xiao, Z.-X. Yang, and F. Wan, "Fractional delay filter based repetitive control for precision tracking: Design and application to a piezoelectric nanopositioning stage," *Mech. Syst. Signal Process.*, vol. 164, p. 108249, 2022, doi: 10.1016/j.ymssp.2021.108249.

[81] C. Jia and R. W. Longman, "An adaptive smooth second-order sliding mode repetitive control method with application to a fast periodic stamping system," *Syst. Control Lett.*, vol. 151, p. 104912, 2021, doi: 10.1016/j.sysconle.2021.104912.

[82] B. M. Yilmaz, E. Tatlicioglu, A. Savran, and M. Alci, "Adaptive fuzzy logic with self-tuned membership functions based repetitive learning control of robotic manipulators," *Appl. Soft Comput.*, vol. 104, p. 107183, 2021, doi: 10.1016/j.asoc.2021.107183.

[83] B. Panomruttanarug, "Position Control of Robotic Manipulator Using Repetitive Control Basedon Inverse Frequency Response Design," *Int. J. Control. Autom. Syst.*, vol. 18, no. 11, pp. 2830–2841, 2020, doi: 10.1007/s12555-019-0518-2.

[84] X. Zhang and Z. Zheng, "Application of Repetitive Control in Electric Spring," *IEEE Access*, vol. 8, pp. 216607–216616, 2020, doi: 10.1109/ACCESS.2020.3041648.

[85] B. A. Francis and W. M. Wonham, "The internal model principle for linear multivariable regulators," *Appl. Math. Optim.*, vol. 2, no. 2, pp. 170–194, 1975, doi: 10.1007/BF01447855.

[86] E. Kurniawan, H. Adinanta, H. G. Harno, J. A. Prakosa, S. Suryadi, and P. Purwowibowo, "On the synthesis of a stable and causal compensator for discrete-time high-order repetitive control systems," *Int. J. Dyn. Control*, vol. 9, no. 2, pp. 727–736, 2021, doi: 10.1007/s40435-020-00695-y.

[87] M. Tomizuka, T.-C. Tsao, and K.-K. Chew, "Analysis and Synthesis of Discrete-Time Repetitive Controllers," *J. Dyn. Syst. Meas. Control.,* vol. 111, 1989, doi: 10.1115/1.3153060.

[88] E. Kurniawan *et al.*, "Design of Fractional Order Odd-Harmonics Repetitive Controller for Discrete-Time Linear Systems with Experimental Validations," *Sensors*, vol. 22, no. 22. 2022, doi: 10.3390/s22228873.

[89] E. Kurniawan, Z. Cao, O. Mahendra, and R. Wardoyo, "A survey on robust Repetitive Control and applications," in *2014 IEEE International Conference on Control System, Computing and Engineering (ICCSCE 2014)*, pp. 524–529, 2014, doi: 10.1109/ICCSCE.2014.7072774.

[90] E. Kurniawan, R. Wardoyo, and E. A. Gojali, "Tracking and robust performance of discrete-time model-based controller," *Proceeding - 2016 Int. Conf. Comput. Control. Informatics its Appl. Recent Prog. Comput. Control. Informatics Data Sci. IC3INA 2016*, no. 4, pp. 28–32, 2017, doi: 10.1109/IC3INA.2016.7863018.

[91] T. Seel, T. Schauer, and J. Raisch, "Iterative Learning Control for Variable Pass Length Systems," *IFAC Proc. Vol.*, vol. 44, no. 1, pp. 4880–4885, 2011, doi: 10.3182/20110828-6-IT-1002.02180.

[92] R. Longman, "Iterative Learning Control and Repetitive Control for Engineering Practice," *Int. J. Control*, vol. 73, pp. 930–954, 2000, doi: 10.1080/002071700405905.